

Supporting Information

Visualization of Vaccine Dynamics with Quantum Dots for Immunotherapy

Junlin Sun⁺, Feng Liu⁺, Wenqian Yu, Dandan Fu, Qunying Jiang, Fengye Mo, Xiuyuan Wang, Tianhui Shi, Fuan Wang, Dai-Wen Pang,* and Xiaoqing Liu**

anie_202111093_sm_miscellaneous_information.pdf

anie_202111093_sm_Movie_S1.avi

anie_202111093_sm_Movie_S2.avi

anie_202111093_sm_Movie_S3.avi

anie_202111093_sm_Movie_S4.avi

anie_202111093_sm_Movie_S5.avi

Table of Contents

Experimental Procedures	2
Figure S1. TEM image of QD@SiO ₂	9
Figure S2. Synthesis of QD@SiO ₂ -Poly.....	10
Figure S3. ¹ H NMR of S-(2-Aminoethylthio)-2-thiopyridine hydrochloride	11
Figure S4. Optimization of the composition of nanovaccines	12
Figure S5. Measurements of CpG and OVA conjugated with QD@SiO ₂ -Poly.....	13
Figure S6. Photoluminescence stability of QD@SiO ₂ with varied pH values	14
Figure S7. Characterization of NIR-I InP/ZnS QD@SiO ₂ -Poly.....	15
Figure S8. Stability of nanovaccines	16
Figure S9. Biocompatibility of of nanovaccines.....	17
Figure S10. Time-dependent cellular uptake of nanovaccines	18
Figure S11. Intracellular colocalization of CpG and OVA.....	19
Figure S12. Photostability of QDs and small molecules	20
Figure S13. Negative control of RAW264.7 cells incubated with nanovaccines	21
Figure S14. Positive control of RAW264.7 cells treated with nanovaccines.....	22
Figure S15. Cytotoxicity of CPZ and dynasore on RAW264.7 cells.....	23
Figure S16. Clathrin-mediated endocytosis of nanovaccines.....	24
Figure S17. Maturation of RAW264.7 cells	25
Figure S18. <i>In vitro</i> immunoactivation by nanovaccines.....	26
Figure S19. Endosomal escape capability of the nanovaccines	27
Figure S20. Flow cytometric plots of T cells in spleen	28
Figure S21. <i>In vivo</i> biodistribution of nanovaccines	29
Figure S22. Hematoxylin-eosin staining of major organs	30
Figure S23. Body weights of the mice in the immunoactivation model.....	31
Figure S24. Body weights of the mice in the prophylactic B16-OVA model	32
Figure S25. Tumor growth plots in the prophylactic B16-OVA model.....	33
Figure S26. Body weights of the mice in the therapeutic B16-OVA model.....	34
Figure S27. Tumor growth plots in the therapeutic B16-OVA model	35
Figure S28. H&E staining and immunohistochemical analysis of tumor slices.....	36
Table S1. Quantum yield measurements	37
References	38

Experimental Procedures

Materials

Tetraethyl orthosilicate (TEOS), 3-mercaptopropyl-trimethoxysilane (MPTS), S-(2-aminoethylthio)-2-thiopyridine hydrochloride thiopyridyl disulfide, 2,2'-azoisobutyronitrile (AIBN), 2-(dimethylamino) ethyl methacrylate (DMAEMA), 2-aminoethylthiol hydrochloride, 4-(2-Hydroxyethyl) piperazine-1 ethanesulfonic acid sodium salt (HEPES), 4-cyano-4-(phenylcarbonothioylthio) pentanoic acid (CPTP), OVA, FITC-labeled OVA and DNase I were purchased from Sigma-Aldrich. Double-distilled water was obtained from Millipore Milli-Q system. CdSe/ZnS QDs and InP/ZnS QD were supplied by Wuhan Jiayuan Quantum and Suzhou Xingshuo Nanotech, respectively. *N*-(3-Dimethylaminopropyl)-*N'*-ethylcarbodiimide hydrochloride (EDCI), Igepal CO-520, 4-dimethylaminopyridine (DMAP), dichloromethane, 1,4-dioxane and neutral red were purchased from Aladdin. Methyl thiazolyl tetrazolium (MTT), DMSO, collagenase I and collagenase IV were obtained from Solarbio. DiO, DAPI and Griess reagent were purchased from Beyotime. Enzyme-linked immunosorbent assay (ELISA) kits of TNF- α , IL-6 and IFN- γ were supplied from Dakewe. Anti-CD40-PE, anti-CD86-FITC and anti-MHC-II-APC were obtained from Sungene Biotech. Anti-CD44-FITC, anti-CD8-PE and anti-CD122-APC were purchased from Miltenyi Biotec. PBS, Dulbecco's modified Eagle's medium (DMEM), penicillin and streptomycin were supplied from HyClone. LysoTracker Green was obtained from Thermo Scientific. Alexa Fluor 488-labeled Tfn was purchased from Jackson ImmunoResearch. EDTA-coated vacutainer tubes were supplied from Wuhan Zhiyuan. Fetal bovine serum (FBS) was purchased from Biological Industries. Anti-PD-1 (RMP1-14) was obtained from BioXCell. DNA was synthesized by Sangon Biotechnology. All other chemicals were supplied by Sinopharm Chemical Reagent Co., Ltd.

Preparation of QD@SiO₂

A two-step synthesis was performed to prepare silica coating of hydrophobic CdSe/ZnS QDs and InP/ZnS QD.^{1,2} Firstly, ethanol solution containing 13 vol % TEOS (155 μ L) was added into QDs (1.4×10^{-8} mol) solution containing toluene (2 mL) and stirred for 24 h at 25 °C. Secondly, Igepal CO-520 (3.5 mL) was dispersed in cyclohexane (45 mL) and stirred for 3 min at 25 °C. Then double-distilled water (500 μ L) and the above QDs solution were added into the microemulsion. The mixtures were stirred for 4 h at 25 °C. Next, ammonia (28 wt %, 500 μ L) and TEOS (300 μ L) were added into the microemulsion, reacting for another 15 h at 25 °C with vigorous stirring. The reaction was terminated by adding additional ethanol (20 mL) and the mixtures were collected by centrifuging with 1.5×10^4 g (Beckman Coulter Allegra X-30R) for 30 min, washed twice by ethanol and redispersed for further use.

Synthesis of sulfhydryl-modified QD@SiO₂ (QD@SiO₂-SH)

The obtained QD@SiO₂ was suspended in anhydrous ethanol (2 mL) containing excess MPTS (20 μ L), and the mixtures were stirred gently for 24 h at 60 °C. After centrifugation (1 \times 10⁴ g), the mixtures were extensively washed with ethanol to purify QD@SiO₂-SH.

Preparation of S-(2-aminoethylthio)-2-thiopyridine hydrochloride

S-(2-aminoethylthio)-2-thiopyridine hydrochloride was synthesized following previous reports.³ Thiopyridyl disulfide (0.441 g) was dissolved in a mixture solution of methanol/acetic acid (3 mL / 0.1 mL). Then, methanol solution (10 mL) containing 2-aminoethylthiol hydrochloride (0.114 g) was added dropwise to the above solution over 30 min. The reaction mixtures were gently stirred for 48 h. After removal of methanol in a rotary evaporator (IKA RV 10), the mixtures were further washed with diethyl ether (5 mL) and redissolved into methanol (1 mL). After that, the mixture solution was precipitated by addition of diethyl ether (20 mL) at -20 °C for 12 h, and the precipitates were collected by vacuum filtration for three times to get the final product.

Synthesis of amino-modified QD@SiO₂ (QD@SiO₂-NH₂)

The above QD@SiO₂-SH was redispersed in the mixture of ethanol (750 μ L) and acetic acid (30 μ L). Then, the suspension was added with the above S-(2-aminoethylthio)-2-thiopyridine hydrochloride (5 mg) and stirred at 25 °C for 48 h. The resultant disulfide-bond containing nanocarriers, denoted as QD@SiO₂-NH₂, were washed exclusively with *N,N*-Dimethylformamide (DMF).

Preparation of CPTP grafted QD@SiO₂ (QD@SiO₂-CPTP)

Firstly, CPTP (30 mg), EDCI (41.1 mg) and DMAP (65.7 mg) was added into dichloromethane (12 mL) and stirred for 30 min at 0 °C. Secondly, the above solution was stirred with the obtained QD@SiO₂-NH₂ at 25 °C for another 16 h and washed exclusively with dichloromethane.

Synthesis of QD@SiO₂-PDMAEMA

As described previously,^{4,5} poly (2-(dimethylamino) ethyl methacrylate) (PDMAEMA)-modified QD@SiO₂ was synthesized by surface-initiated reversible addition-fragmentation chain transfer (RAFT) polymerization using QD@SiO₂-CPTP as a chain transfer agent (CTA) and AIBN as an initiator in the presence of DMAEMA as the monomer. DMAEMA (32 μ L) was mixed with 1,4-dioxane (4 mL) solution containing CTA and AIBN (1 mg) in a glass round-

bottom flask with gentle stirring, and purged with argon for 30 min. The mixtures were then transferred to a glove box under nitrogen purge. The polymerization was carried out at 70 °C for 8 h. The obtained mixtures were centrifuged at 1.5×10^4 g for 25 min and rinsed with ethanol for three times. After removal of ethanol in a rotary evaporator, the obtained product was finally dissolved in HEPES (10 mM, pH 7.4) buffer, leaving only a trace of insoluble material behind.

Preparation and characterization of QD@SiO₂-Poly-CpG-OVA

OVA and CpG (CpG 1826: 5'-TCC ATG ACG TTC CTG ACG TT-3') were incubated with QD@SiO₂-Poly at feed molar ratio of 100/100/1 in HEPES buffer for 30 min with gentle stirring, and then centrifuged at 1.5×10^4 g for 20 min. The amount of OVA absorbed onto QD@SiO₂-Poly was determined *via* the Bradford method with free OVA as the protein standard. The amount of OVA absorbed on QD@SiO₂-Poly was measured by UV-Vis spectrophotometer (Shimadzu UV-2600). The amount of CpG (labeled with Quasar, Cy5 or FITC) absorbed on QD@SiO₂-Poly was determined by spectrofluorometer FS5 (Edinburgh Instruments). The precipitation was redispersed in PBS for further experiments. The surface morphology of QD@SiO₂ was investigated by transmission electron microscopy (TEM, Hitachi HT-7700). The size and zeta potential analysis were detected by dynamic light scattering (DLS, Malvern Instruments Nano-ZS90). The fluorescence property of QD@SiO₂-Poly was measured by spectrofluorometer FS5.

***In vitro* drug release**

In order to investigate the *in vivo* simulated release of OVA and CpG in the confined system, the PBS media was partially changed every day. The cumulative release of OVA and CpG was studied at 37 °C in 5 mL PBS for 5 days. At the predetermined time intervals, an aliquot 500 μ L of PBS was collected and centrifuged for analyzing the supernatant. To maintain a constant volume of PBS media, the remaining 4.5 mL PBS media was supplemented with 500 μ L of fresh PBS.

pH-dependent hemolysis assay

The capacity of nanovaccines to promote pH-dependent disruption of lipid bilayer membranes was assessed by a RBC hemolysis assay as previously described.⁶ Blood samples stabilized in EDTA-coated vacutainer tubes were obtained from C57BL/6j mice (Hubei Center for Disease Control and Prevention (Wuhan, China)). RBCs were isolated from obtained serum by centrifugation at 1×10^4 g for 10 min and washed three times until the supernatant turned colorless. Then redispersed erythrocyte with different pH values (varying from 5.2 to 7.6, 200

μL) were added into QD@SiO₂-Poly-CpG-OVA (800 μL with corresponding pH, 50 $\mu\text{g}/\text{mL}$). RBCs solution dispersed in H₂O/PBS (800 μL) was treated as positive/negative control. After 1 h incubation at 37 °C, the above mixtures were centrifuged at $1 \times 10^4 g$ for 10 min and the absorbance of supernatant was determined at 577 nm (corrected for background absorbance at 655 nm). Three replicates were proceeded for each treatment group.

Cell culture

RAW264.7 cells and B16-OVA cells (Cell Bank of Chinese Academy of Sciences, Shanghai) were grown in the DMEM added with 10% FBS, penicillin (100 units/mL) and streptomycin (100 mg/mL) at 37 °C in a humidified 5% CO₂-containing atmosphere (ESCO).

MTT assays

Cells were seeded in 96-well plates with a density of 5×10^3 cells/well (total volume of 200 $\mu\text{L}/\text{well}$). After 12 h attachment, the as-prepared QD@SiO₂-Poly and QD@SiO₂-Poly-CpG-OVA, at the various concentrations (0, 2, 5, 10, 20, 50, 80 and 100 $\mu\text{g}/\text{mL}$), were added for further incubation of 48 h. To determine cell toxicity, 100 μL of MTT solution (0.5 mg/mL) was added into each well and incubated for 4 h. Afterward, the MTT solution was removed and the cells were lysed by the addition of DMSO (150 μL). Absorbance values of formazan were determined at 490 nm (corrected for background absorbance at 630 nm, Thermo Scientific Multiskan Go). Four replicates were proceeded for each treatment group.

Hemolysis compatibility assays

To determine hemolysis compatibility, blood samples stabilized in EDTA-coated vacutainer tubes were obtained from the mice. RBCs were isolated from the obtained serum by centrifugation at $1 \times 10^4 g$ for 10 min and rinsed three times until the supernatant turned colorless. Then redispersed erythrocyte (200 μL) were added into QD@SiO₂-Poly-CpG-OVA (800 μL) with the final concentration of 2, 5, 10, 20, 50, 80 and 100 $\mu\text{g}/\text{mL}$. RBCs solution dispersed in H₂O/PBS (800 μL) was treated as positive/negative control. After 4 h incubation at 37 °C, the above mixture was centrifuged at $1 \times 10^4 g$ for 10 min and the absorbance of supernatant was determined at 577 nm (corrected for background absorbance at 655 nm). Four replicates were proceeded for each treatment group.

Cytokines assays *in vitro*

Cells were seeded in 6-well plates with a density of 5×10^4 cells/well (total volume of 1 mL/well). After 12 h attachment, the cells were washed with PBS before incubation with indicated materials for 8 h (TNF- α) or 24 h (IL-6). The supernatants were collected and stored

at -80 °C (Haier Bio-Medical) until use. The levels of TNF- α and IL-6 in the supernatants were determined by ELISA following protocols recommended by the manufacturer.

Confocal fluorescence imaging

Cells were incubated on a glass-bottomed Petri dish (Nest) and treated with prechilled nanovaccines at 4 °C for 10 min, and then shifted to 37 °C for further real time observation. The Petri dish was placed onto a temperature-controlled chamber (INUBG2-PI) of the microscope stage. Time-lapse live-cell images were performed by a spinning-disk confocal microscope system (Revolution XD, Andor) equipped with a heated 100 \times objective (NA = 1.40), a motorized invert microscope (TiE, Nikon), a Nipkow disk type confocal unit (CSU-X1, Yokogawa) and an Emission filter wheel (Sutter Instruments). Fluorescence signals were detected *via* the EMCCD (Andor iXon Ultra 897) to simultaneously image multiple targets with different colors.

Image analysis

The signals of nanovaccines and dyes were tracked *via* Imaging-Pro Plus (Media Cybernetics). Only integral trajectories in the focal plane were used in quantitative SPT analysis. The MSD of each trajectory was calculated for each time interval by the user-written program with MATLAB (MathWorks). The motion mode was determined by fitting MSD and Δt to the following functions:

Free diffusion: $MSD = 4D\Delta t$

Restricted diffusion: $MSD = 4D\Delta t^\alpha$ ($\alpha < 1$)

Directed diffusion: $MSD = 4D\Delta t + (V\Delta t)^2$

D represents the diffusion coefficient and V represents the mean velocity.

Morphology observation

1×10^4 RAW264.7 cells were seeded in 35 mm culture dishes overnight. The cells were incubated with the nanovaccines for 24 h. The cells were further washed using PBS and fixed with paraformaldehyde (4%) for 15 min at room temperature. Then, the cells were stained with DPAI and DiO (cell membranes labeling) for 25 min at room temperature for fluorescence imaging.

NO production

Cells were seeded in 96-well plates with a density of 5×10^4 cells/well. After 12 h attachment, cells were incubated with different formulations at 50 $\mu\text{g/mL}$ of QD@SiO₂-Poly for 24 h,

respectively. Cells were washed by PBS for 3 times and added with equal volumes of Griess reagent. Then, the absorbance at 540 nm was determined.

Phagocytosis activity assay

Cells were cultured in 96-well plates with a density of 2×10^4 cells/well overnight. Then, cells were treated with different formulations at 50 $\mu\text{g/mL}$ of QD@SiO₂-Poly for 24 h, respectively. Cells were washed by PBS three times and incubated with 100 μL of 0.1% neutral red (dissolved in PBS solution) for 30 min. After washing three times with PBS, 150 μL of cell lysis solution ($V_{\text{acetic acid}}/V_{\text{ethanol}} = 1/1$) was added at 37 °C for 1 h. The absorbance at 540 nm was measured.

In vivo imaging and immunogenicity study

Female C57BL/6j mice of 6–8 weeks were purchased from Hubei Center for Disease Control and Prevention (Wuhan, China). All animal experiments were performed in accordance with the National Institute of Health Guide for the Care and Use of Laboratory Animals and approved by Use Committee of the Animal Experiment Center/Animal Biosafety Level-III Laboratory of Wuhan University (license number: WP2020-08048).

To monitor lymphatic drainage of the nanovaccines, C57BL/6j mice of 6–8 weeks were randomly divided into several groups (the CpG were labeled with Quasar). C57BL/6j mice were s.c. injected with the indicated materials at the tail base, respectively. The mice were used for *in vivo* imaging from 10 to 50 min (PE Spectrum & Quantum FX). At 24 h post injection, major organs and LNs (axillary, inguinal and popliteal LNs) of mice injected with nanovaccines were harvested for *ex vivo* imaging. The ILNs were smashed, treated with collagenase I (1 mg/mL), collagenase IV (0.1 mg/mL) and DNase I (0.1 mg/mL) for 1 h at 37 °C to prepare single cells.⁷ The cells were filtered through a 40- μm strainer to remove tissue debris and counted the total cell numbers. Additionally, InP/ZnS QDs-based nanovaccines were also performed for *in vivo* imaging from 30 min to 72 h.

To estimate immunogenicity study of nanovaccines, the mice were divided into 6 groups with four mice per group. Mice were vaccinated with 50 μL of different formulations at 4 mg/kg of QD@SiO₂-Poly, or equivalent, on days 0, 7, 14 and 21, and the sera were collected on day 30. The proinflammatory cytokines from sera were determined by using ELISA kits following standard protocols (TNF- α , IL-6 and IFN- γ). Single cells collected from ILNs were stained with anti-CD40-PE, anti-CD86-FITC and anti-MHC-II-APC for analyzing APCs. Splenocytes (following the same preparation as ILNs) harvested from the mice were stained with anti-CD44-FITC, anti-CD8-PE and anti-CD122-APC for analyzing CD8⁺ central memory T cells. The rest splenocytes (5×10^4 cells/well) were restimulated with OVA (40 $\mu\text{g/mL}$) for 60 h in 96-

well plates. Then, the cells were washed several times with PBS to completely remove residual OVA and then cultured together with target cells (B16-OVA) at different effector cells/target cells ratios (60/1, 80/1 and 100/1). After incubation for 4 h, the suspensions were collected to detect level of specific lysis of target cells by effective cells using MTT assays, which indicated the level of specific lysis of target cells by effective cells. The percentage of specific lysis was calculated according to $\text{specific lysis\%} = (\text{test release} - \text{effector cell release}) / (\text{maximum release} - \text{spontaneous release}) \times 100\%$ ($n = 4$).

***In vivo* prophylactic and therapeutic study for tumor suppression**

To study prophylactic efficacy, C57BL/6j mice were s.c. injected at the tail base with different formulations of QD@SiO₂-Poly (4 mg/kg, 50 μ L), or equivalent, on days 0, 7, 14 and 21. On days 30, mice were s.c. inoculated with 4×10^4 B16-OVA cells on the right flank. Tumor volumes were calculated as $(\text{length} \times \text{width}^2 / 2)$ and measured every 2 days. Mice were euthanized if tumor volumes were above 1×10^3 mm³, or tumors became ulcerated.

To investigate therapeutic efficacy, C57BL/6j mice were inoculated with 4×10^4 B16-OVA cells s.c. on day 0. Then mice were s.c. injected at the tail base with QD@SiO₂-Poly-CpG-OVA (4 mg/kg, 50 μ L) and on days 4, 7, 10, 13 and 16. Anti-PD-1 (10 μ g) was administered i.v. on the same days. Tumor volumes were measured every other day. Tumor tissues and major organs (heart, liver, spleen, lung and kidney) were harvested on days 19 and used for H&E staining and IHC analysis.

Statistical Analysis

All the data were presented as mean \pm SD. Statistical analysis was calculated by one-way ANOVA with the Bonferroni post hoc test using IBM SPSS Statistics 19. Statistical significance is indicated as ns, not significant, * $P < 0.05$, ** $P < 0.01$ and *** $P < 0.001$.

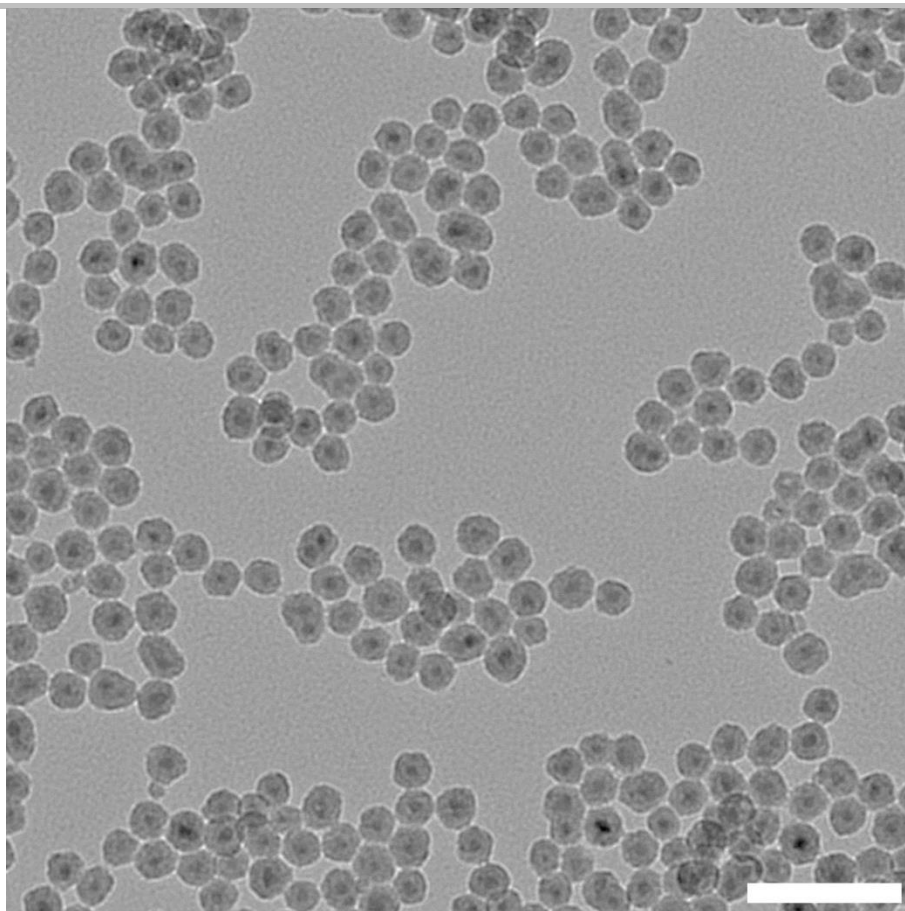


Figure S1. TEM image of QD@SiO₂. Scale bar is 100 nm.

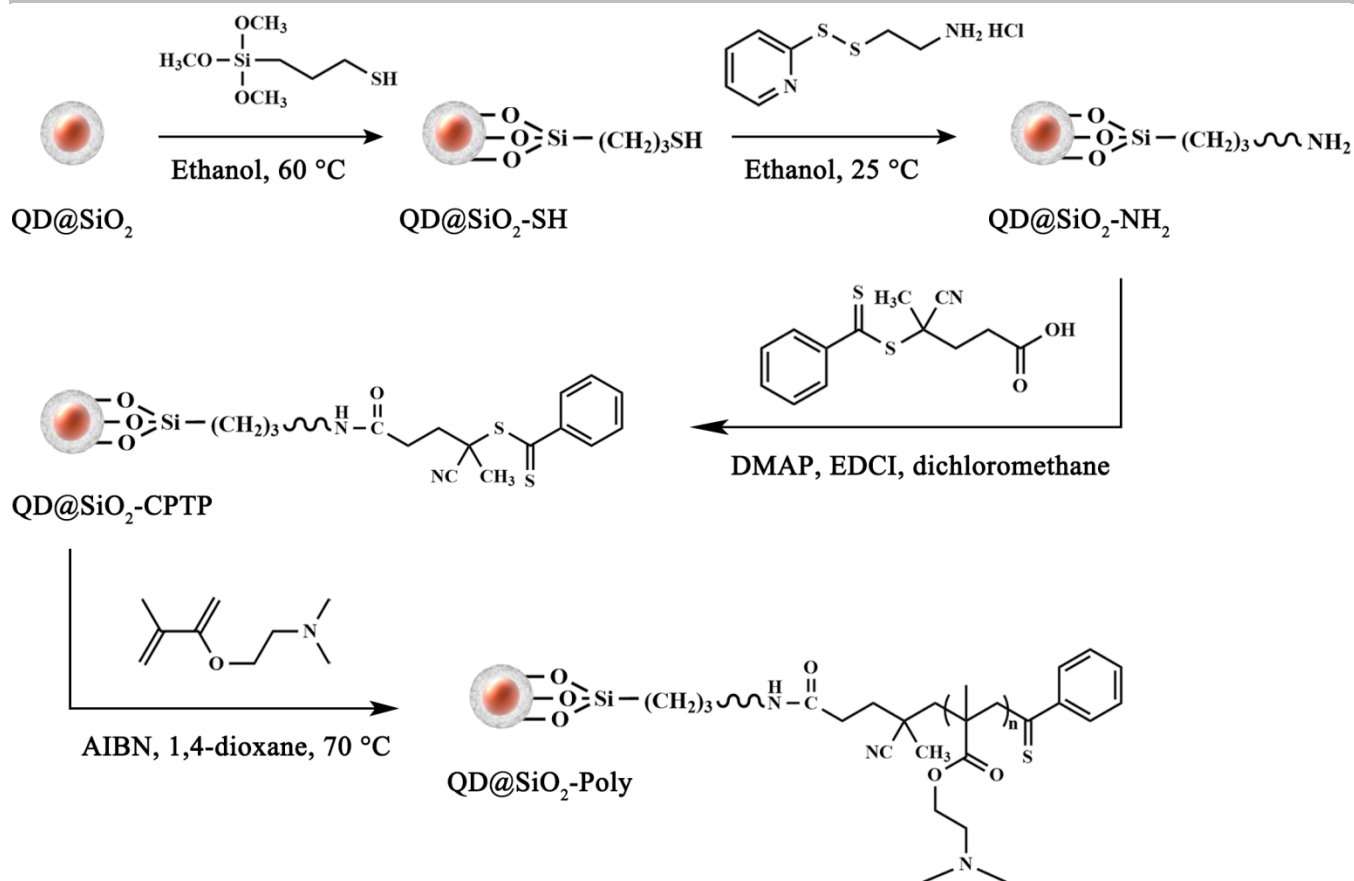


Figure S2. Surface-initiated RAFT synthesis of QD@SiO₂-Poly.

Silica coated QDs (QD@SiO₂) were synthesized *via* a classical microemulsion method.^{1,2} Transmission electron microscope (TEM) images of QD@SiO₂ showed that the average diameter of QD@SiO₂ was 24.3 nm, and almost every single QD was well isolated in the middle of SiO₂ sphere (Figure S1). Cationic polyelectrolytes were modified onto the surface of QD@SiO₂ through reversible addition-fragmentation chain transfer (RAFT) polymerization *via* stepwise functionalization (Figure S2). Following sulfhydrylation of QD@SiO₂ with 3-mercaptopropyl-trimethoxysilane, the obtained QD@SiO₂-SH was aminated with S-(2-aminoethylthio)-2-thiopyridine hydrochloride (Figure S3, ¹H NMR) to produce QD@SiO₂-NH₂. After grafting with a chain transfer agent 4-cyano-4-(phenylcarbonothioylthio) pentanoic acid (CPTP) for synthesizing QD@SiO₂-CPTP, surface-initiated RAFT polymerization proceeded in the presence of 2,2'-azoisobutyronitrile (AIBN) as the initiator and 2-(dimethylamino) ethyl methacrylate as the monomer to form cationic polymer (poly (2-(dimethylamino) ethyl methacrylate), PDMAEMA)-modified QDs (QD@SiO₂-Poly).

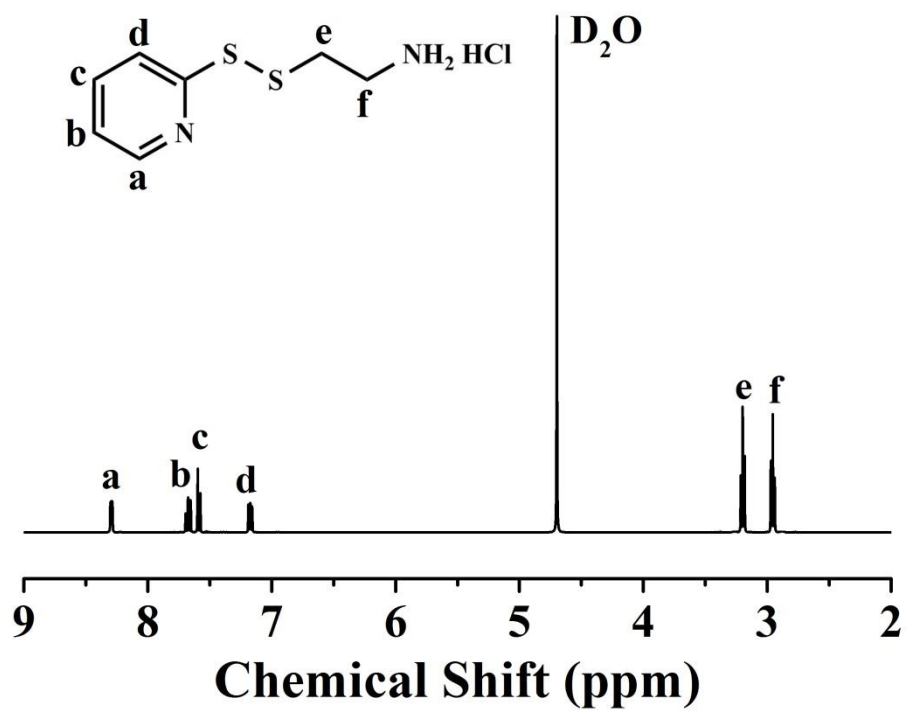


Figure S3. ^1H NMR spectra of S-(2-Aminoethylthio)-2-thiopyridine hydrochloride.

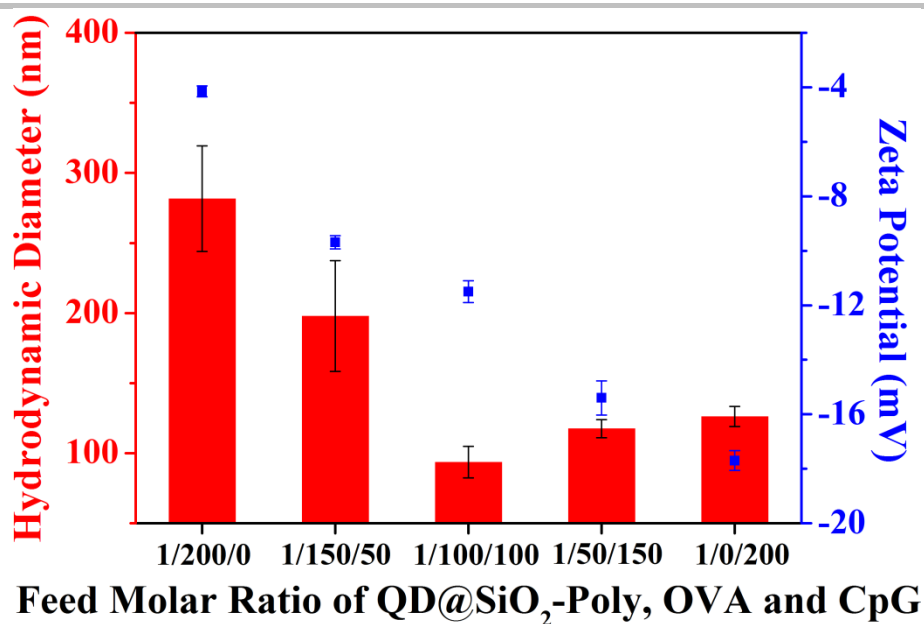


Figure S4. The optimization of feed molar ratio of positively charged QD@SiO₂-Poly, and negatively charged OVA and CpG on hydrodynamic diameter and zeta potential of QD@SiO₂-Poly-CpG-OVA conjugates. The PDI of the ratio of 1/200/0 and 1/150/50 was 0.76 and 0.45, respectively (easily aggregated). The PDI of the ratio of 1/100/100, 1/50/150 and 1/0/200 was all below 0.3. ($n = 4$, mean \pm SD).

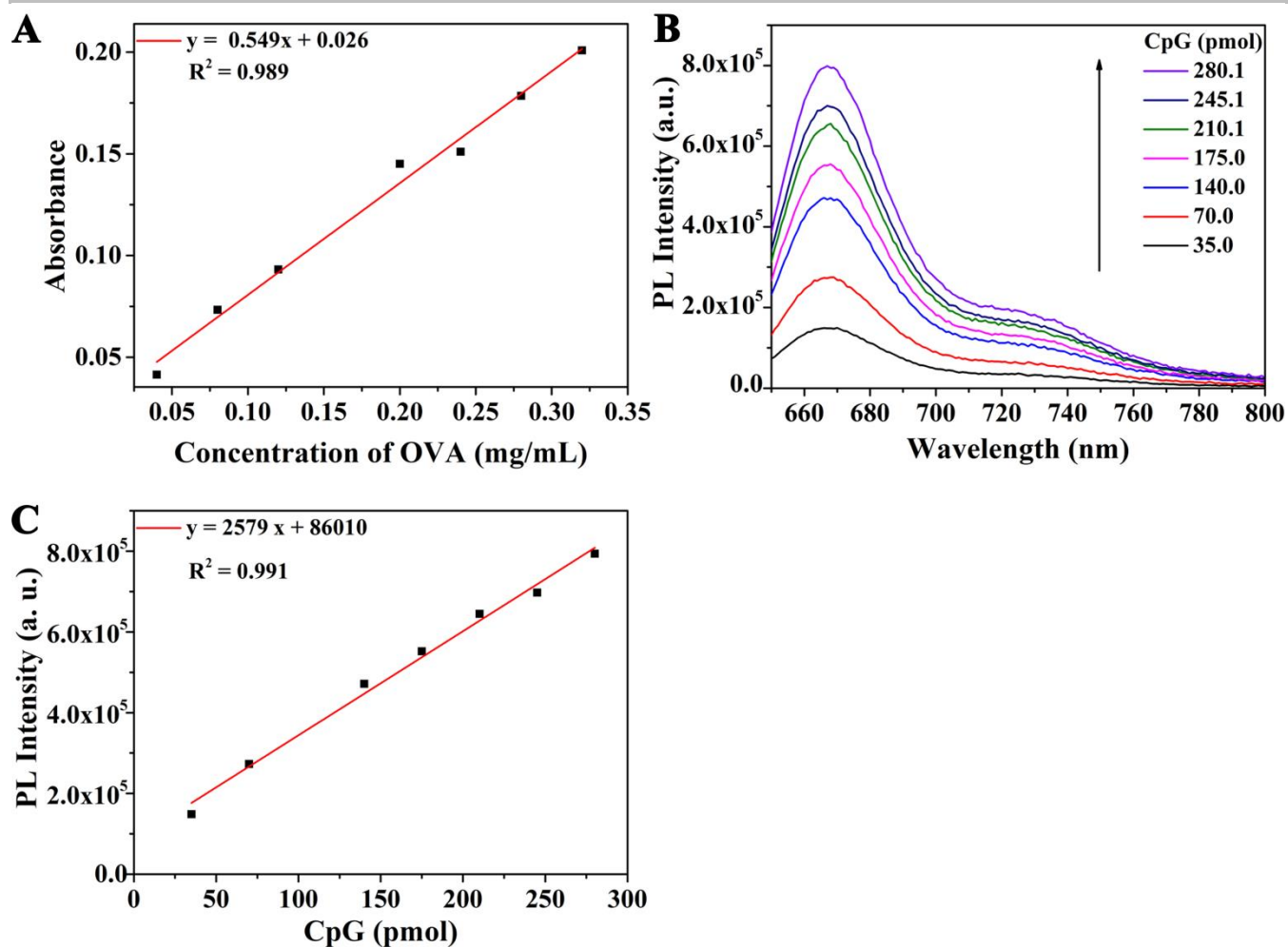


Figure S5. (A) Standard concentration curve of OVA measured by Bradford method. (B) Fluorescence spectra of Quasar-CpG with varied concentrations. (C) PL intensity of the corresponding peak of each spectrum in (B). The calculated conjugated OVA and CpG molecules with QD@SiO₂-Poly were 575 and 803, respectively.

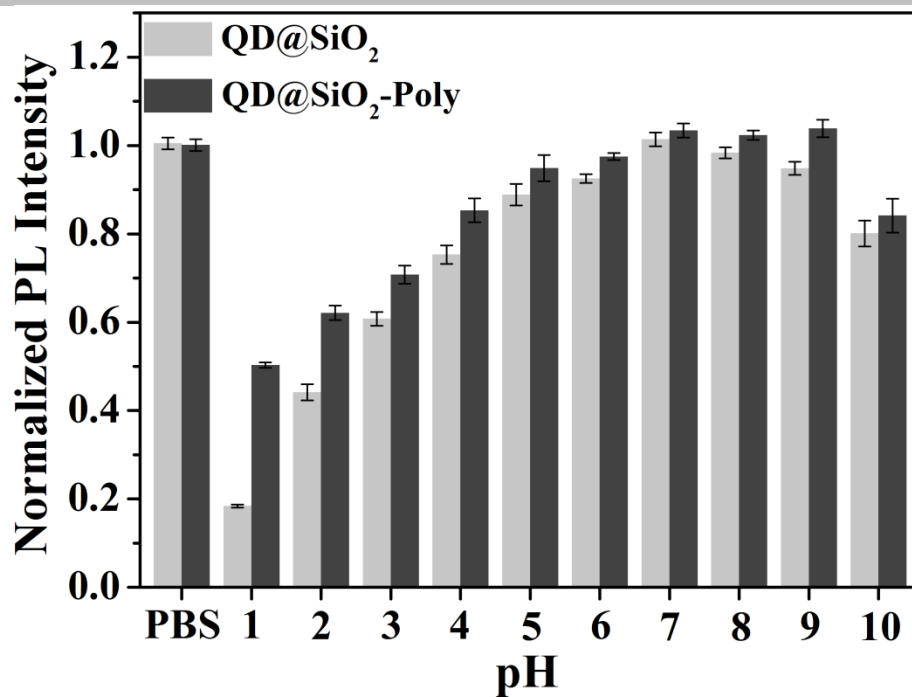


Figure S6. Photoluminescence stability of QD@SiO₂ and QD@SiO₂-Poly in aqueous solutions with pH values ranging from 1 to 10 for 24 h ($n = 3$, mean \pm SD).

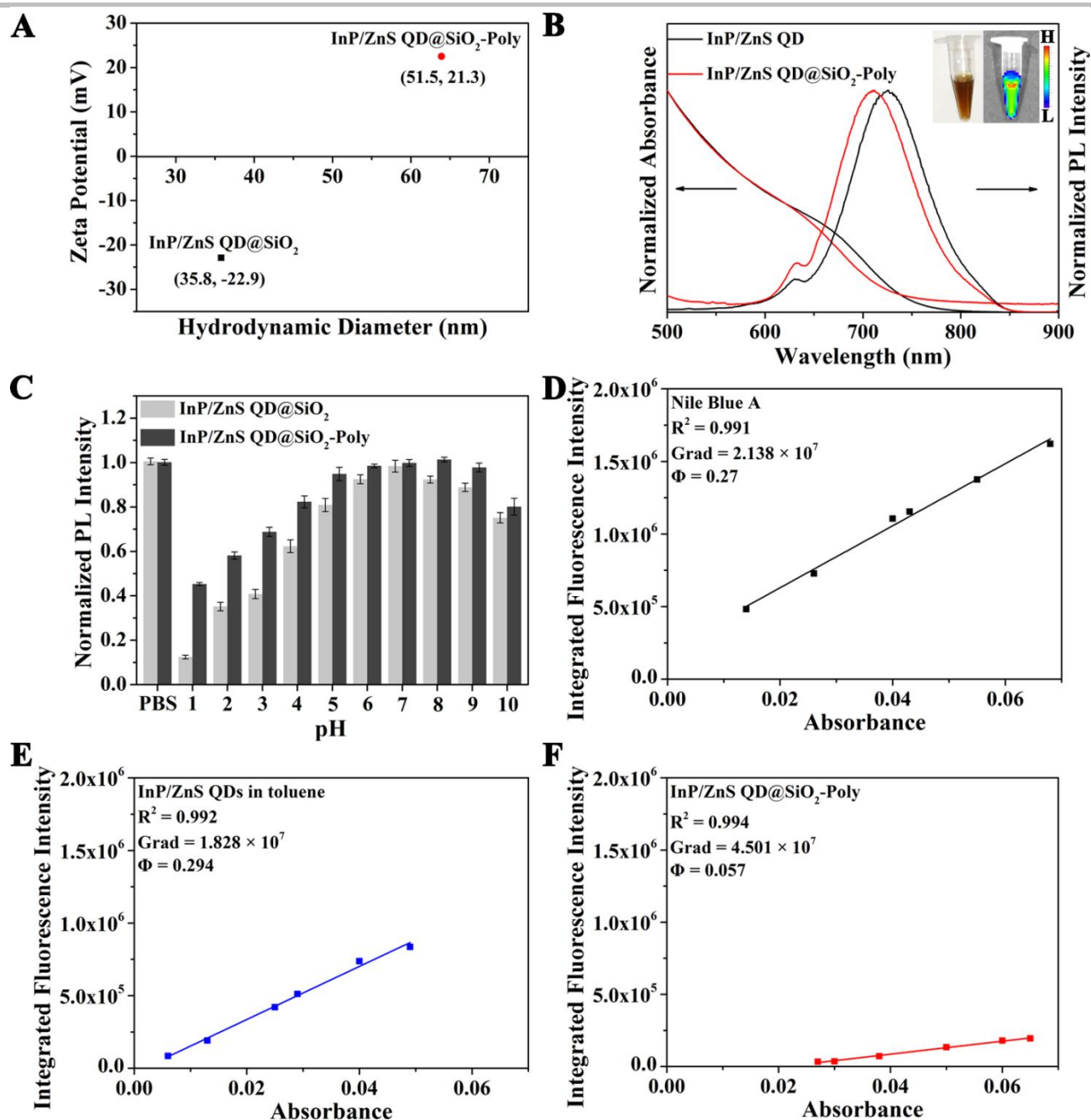


Figure S7. Characterization of InP/ZnS QD@SiO₂-Poly. (A) Mean hydrodynamic sizes and zeta potential of QD@SiO₂ and QD@SiO₂-Poly suspended in water ($n = 3$, mean \pm SD, PDI < 0.3). (B) Visible light absorption and PL spectra of hydrophobic QDs and QD@SiO₂-Poly. Inset: photographs of QD@SiO₂-Poly in water under daylight (left) and 430 nm xenon excitation (right). (C) Normalized fluorescence intensity of the indicated materials with pH values ranging from 1 to 10 and PBS solutions at 24 h, respectively. (D–F) Quantum yields of Nile blue A (D, in methanol, standard), hydrophobic QDs (E) and QD@SiO₂-Poly (F), respectively.

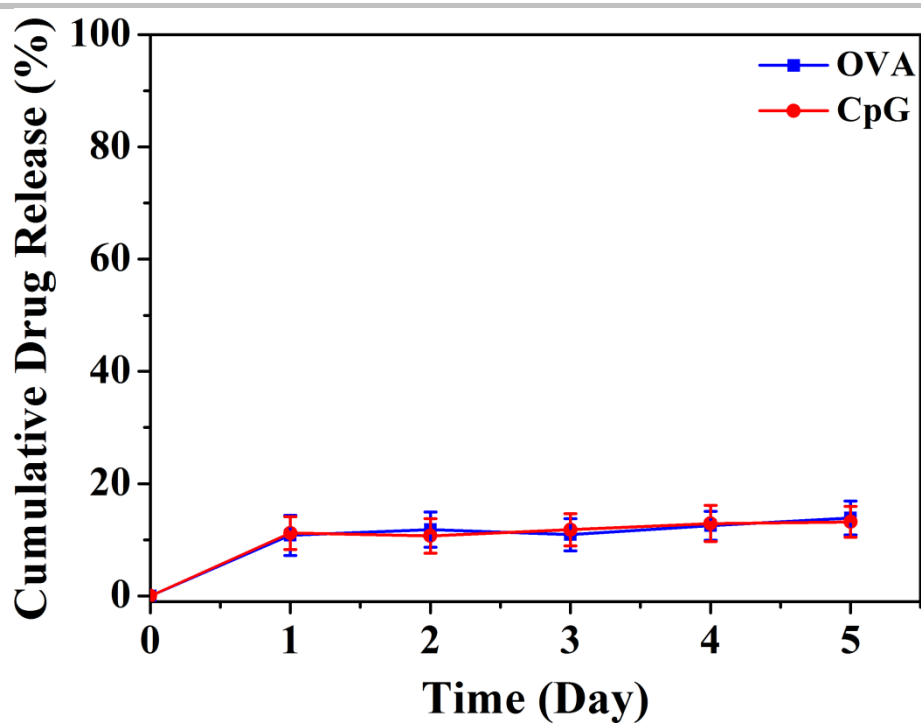


Figure S8. The stability of nanovaccine in PBS (pH 7.4) for varied durations at 37 °C ($n = 3$, mean \pm SD).

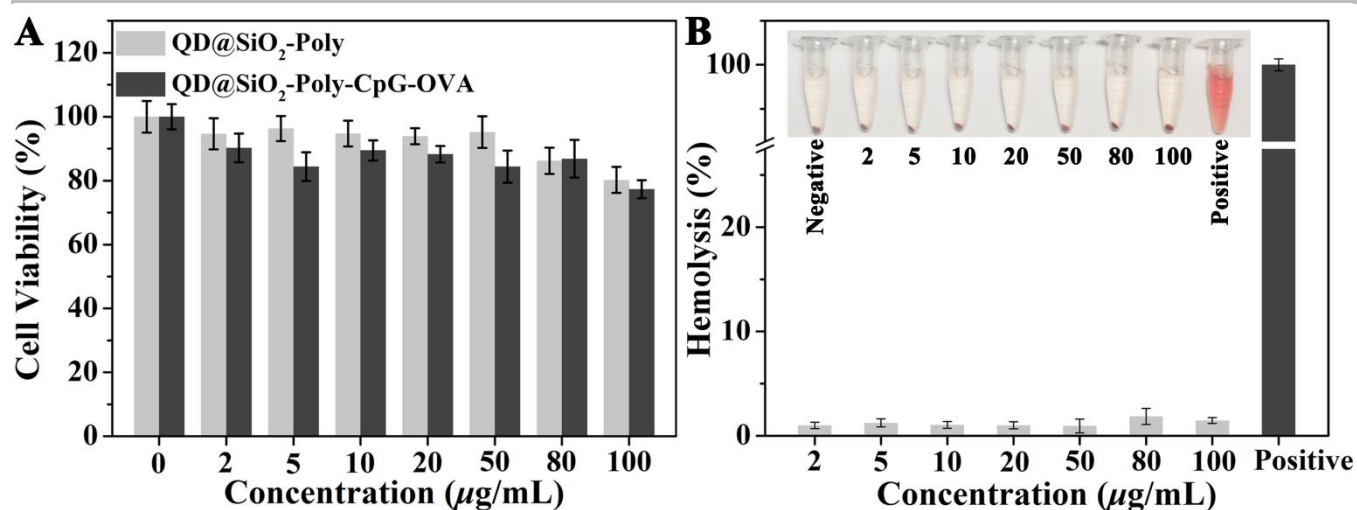


Figure S9. Biocompatibility of QD@SiO₂-Poly and QD@SiO₂-Poly-CpG-OVA. (A) Cytotoxicity testing results of QD@SiO₂-Poly and QD@SiO₂-Poly-CpG-OVA conjugates against RAW264.7 cells by MTT assays. (B) Hemolytic activity of QD@SiO₂-Poly-CpG-OVA at pH 7.4 ($n = 4$, mean \pm SD).

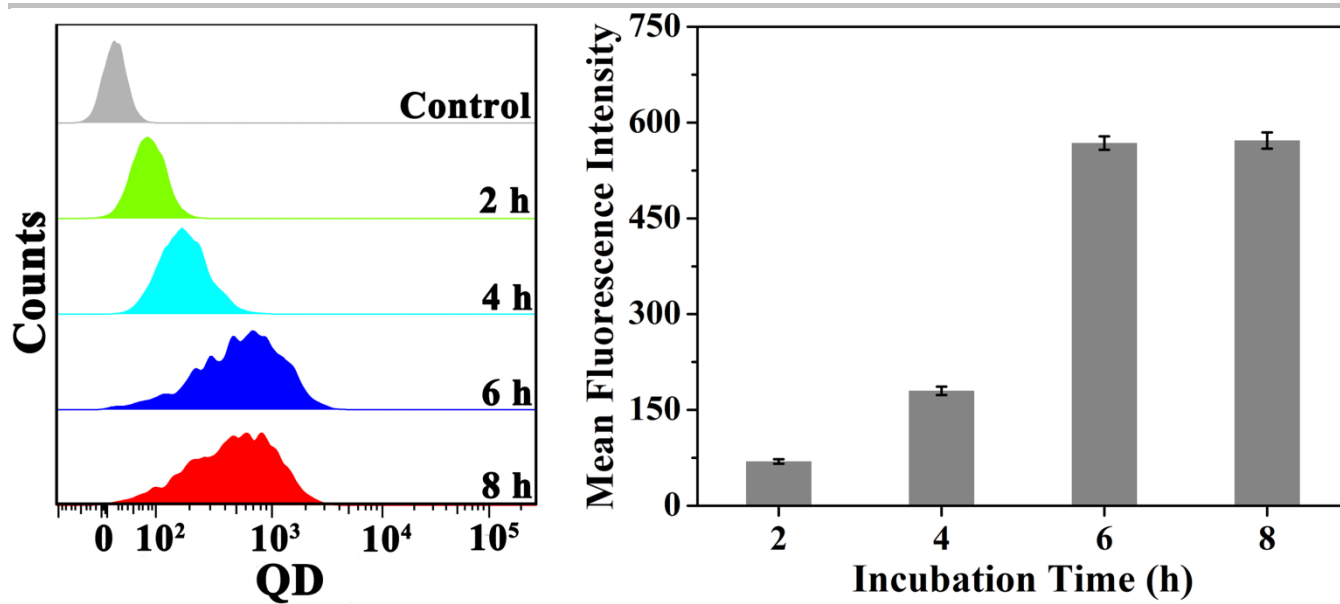


Figure S10. Flow cytometry analysis of time-dependent intracellular delivery of QD@SiO₂-Poly-CpG-OVA (50 µg/mL).

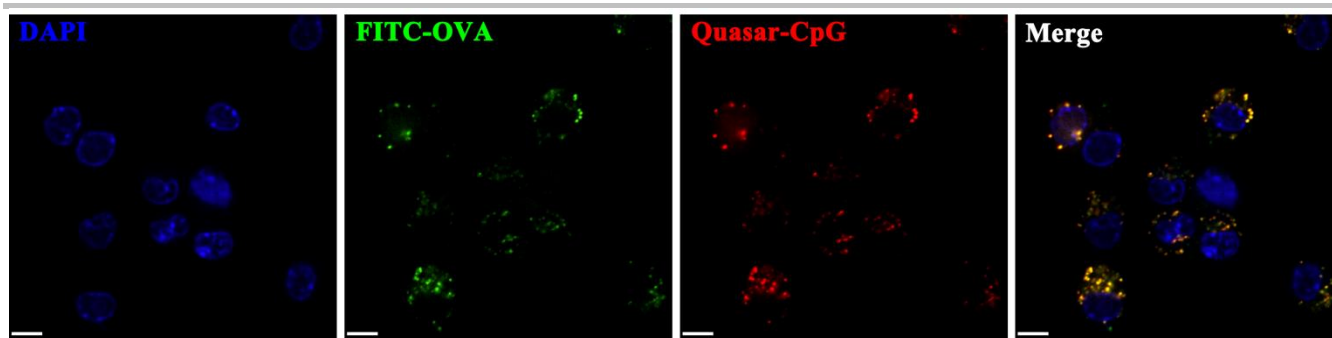


Figure S11. Confocal images of RAW264.7 cells treated with the nanovaccines for 8 h at 37 °C. The OVA was modified by FITC and CpG were labeled with Quasar (50 $\mu\text{g}/\text{mL}$). Scale bar is 10 μm .

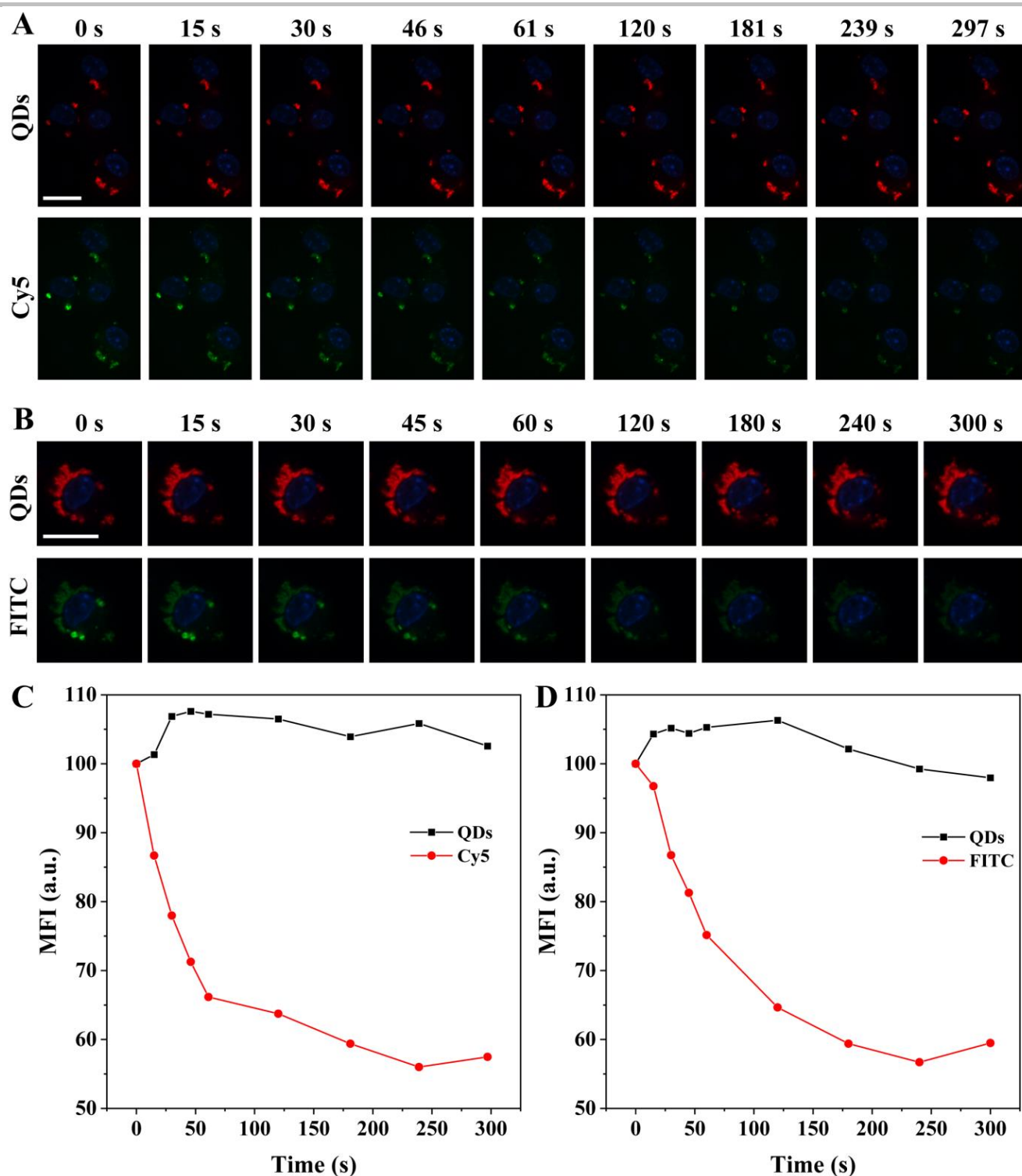


Figure S12. Photostability investigation of the synthetic QDs and small molecules (Cy5 and FITC). (A and B) Snapshots of QD@SiO₂-Poly-CpG-OVA in RAW264.7 cells. Cy5-CpG and FITC-CpG were used in (A) and (B), respectively. Scale bar is 15 μ m. (C and D) Time-dependent MFI of QDs, Cy5 and FITC obtained in (A and B).

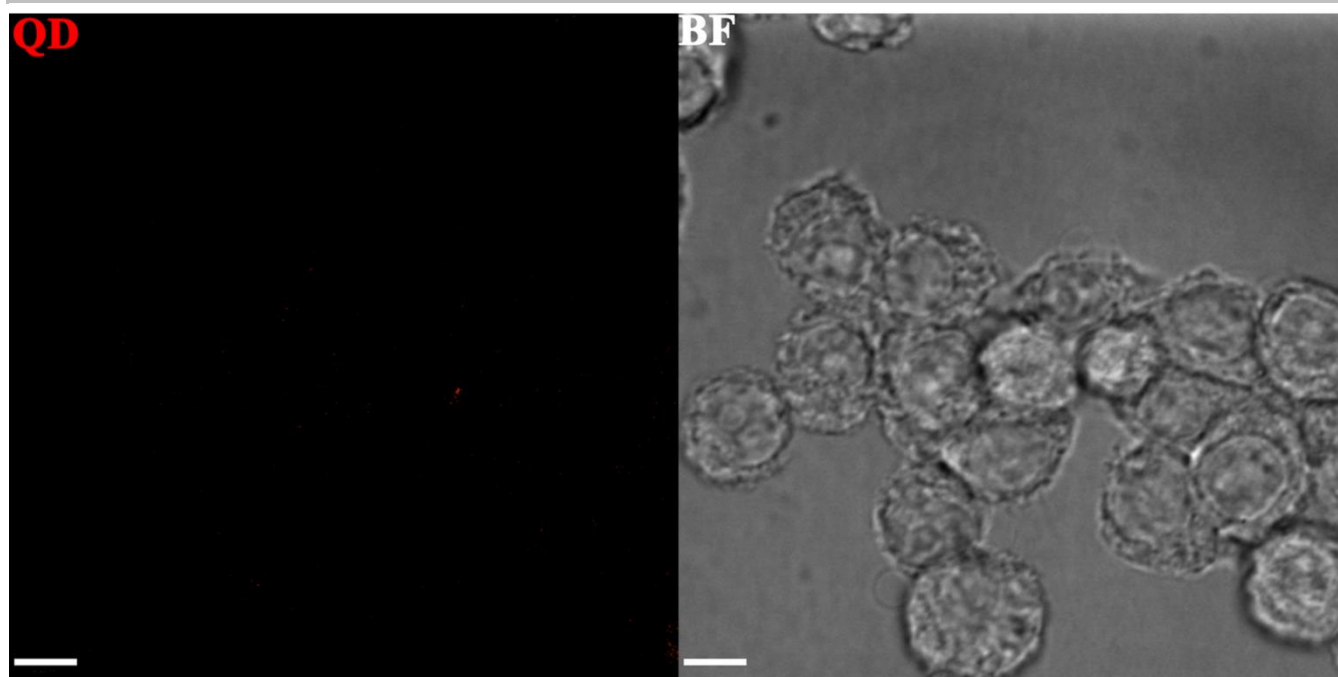


Figure S13. Confocal images of RAW264.7 cells incubated with the prechilled nanovaccines at 4 °C for 10 min after several times wash by PBS. Scale bar is 10 μm .

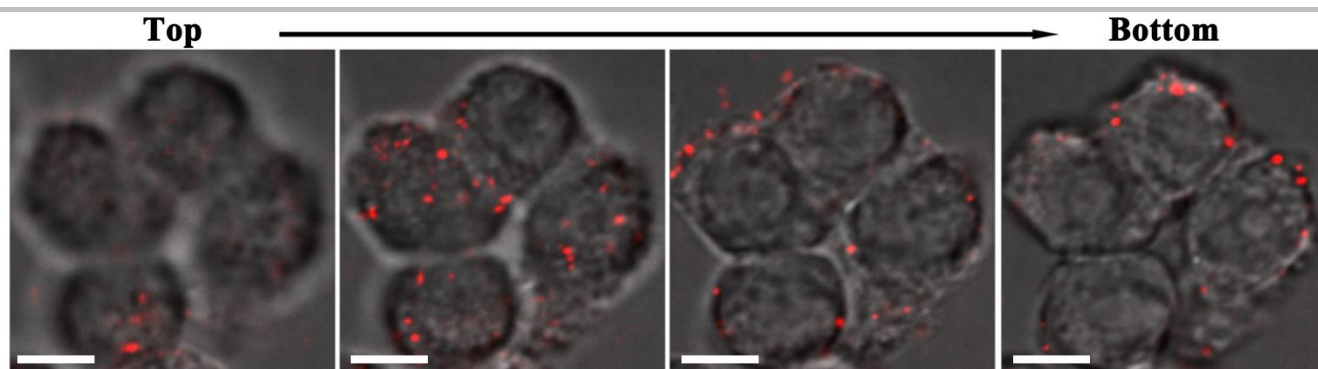


Figure S14. Confocal images of RAW264.7 cells treated with the prechilled nanovaccines at 4 °C for 10 min without wash by PBS (Z plane slices from top to bottom). Scale bar is 10 μm .

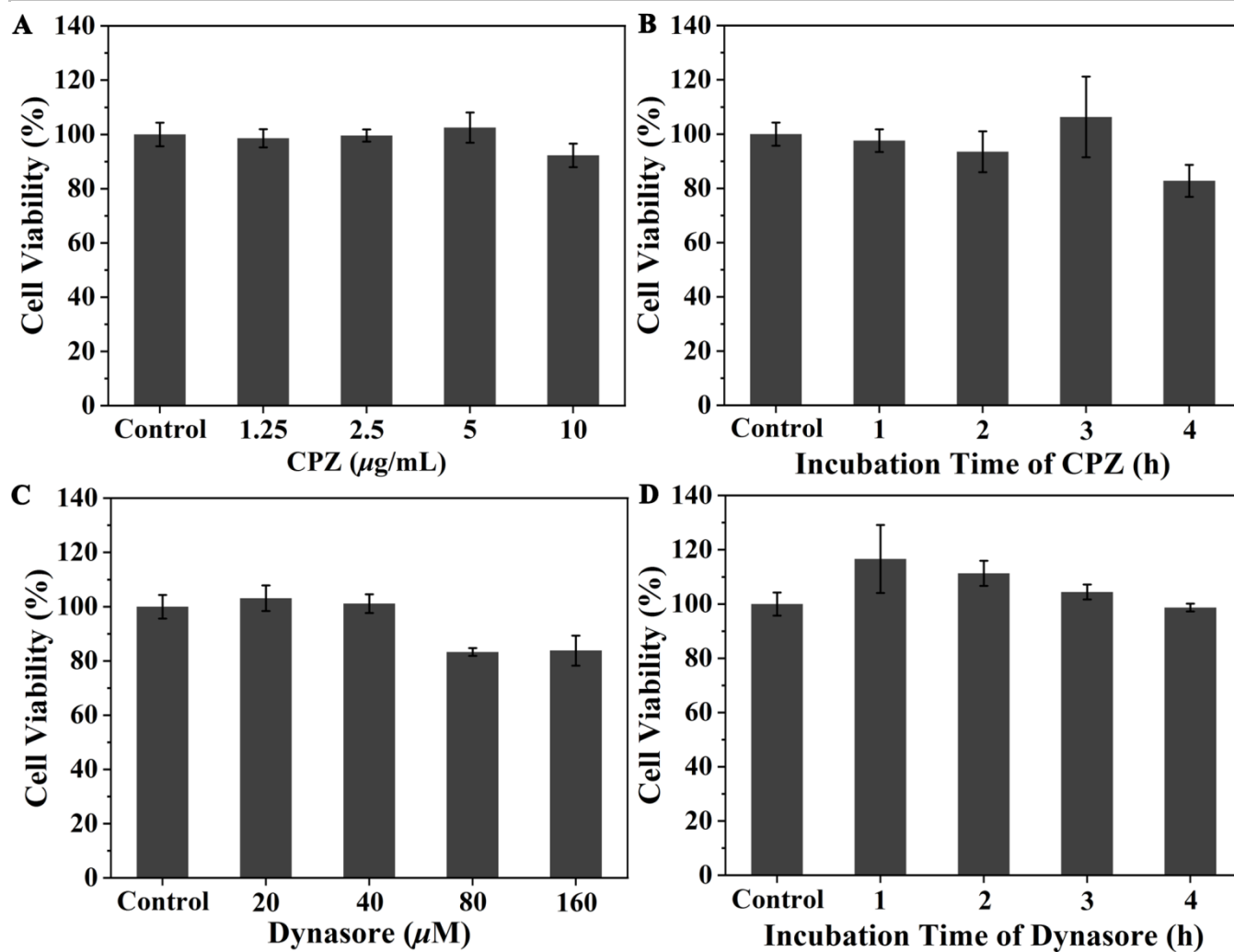


Figure S15. Cell viability determined by MTT assays of RAW264.7 cells incubated with different concentrations of CPZ (A) and dynasore (C) for 30 min, respectively. Cell viability of RAW264.7 cells treated with appropriate concentration of CPZ (10 $\mu\text{g/mL}$, B) and dynasore (40 μM , D) for incubating at different time ($n = 4$, mean \pm SD), respectively.

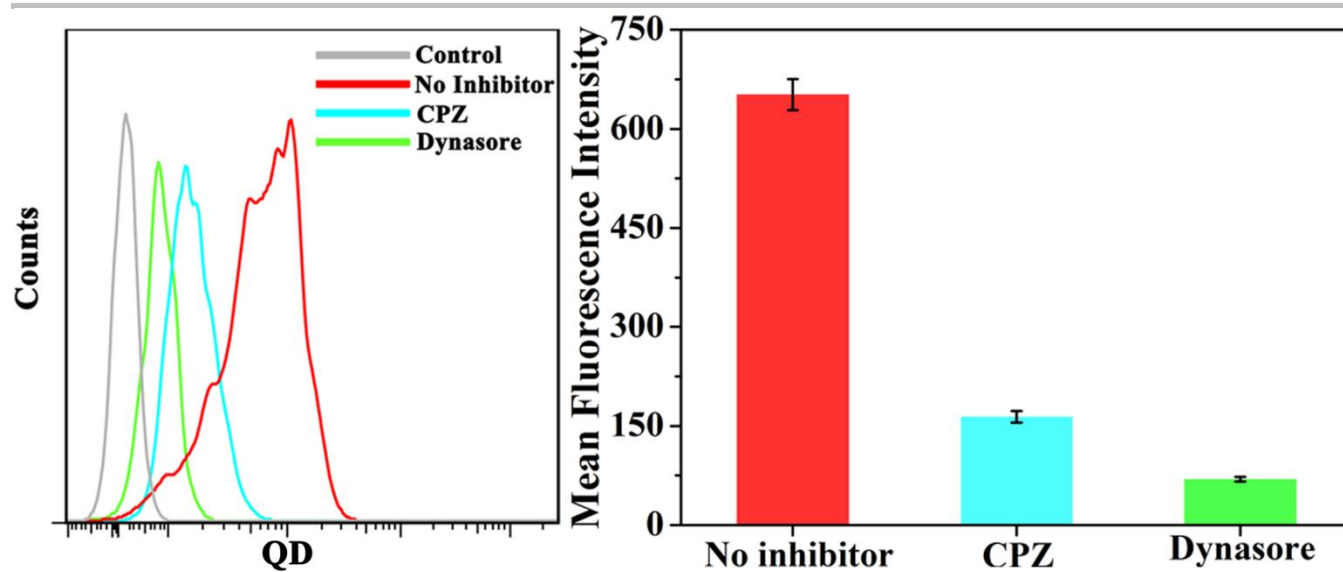


Figure S16. Flow cytometry analysis of control group and inhibitor-treated groups ($n = 3$, mean \pm SD).

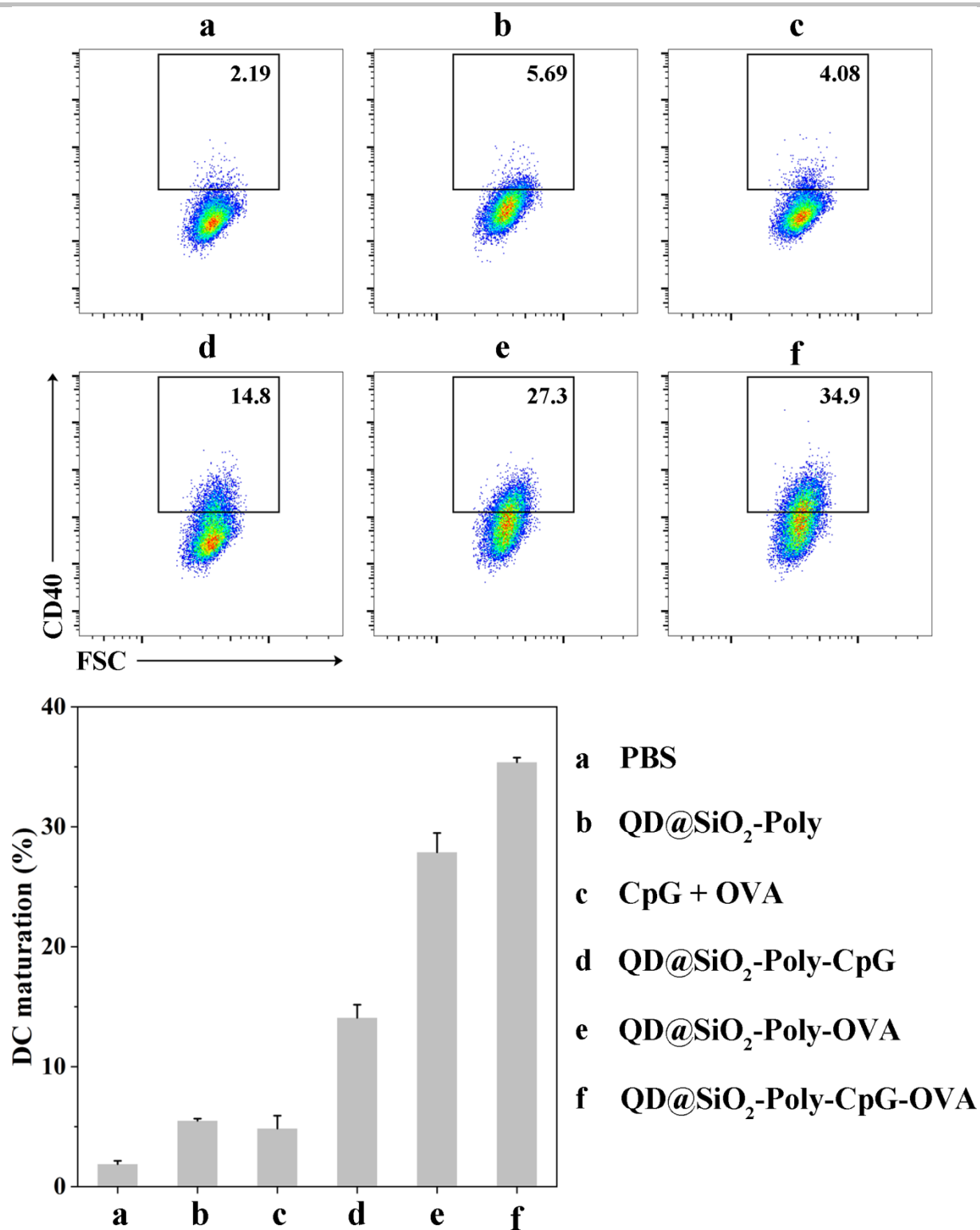


Figure S17. Flow cytometry analysis on the maturation of RAW264.7 cells (CD40⁺ cells).

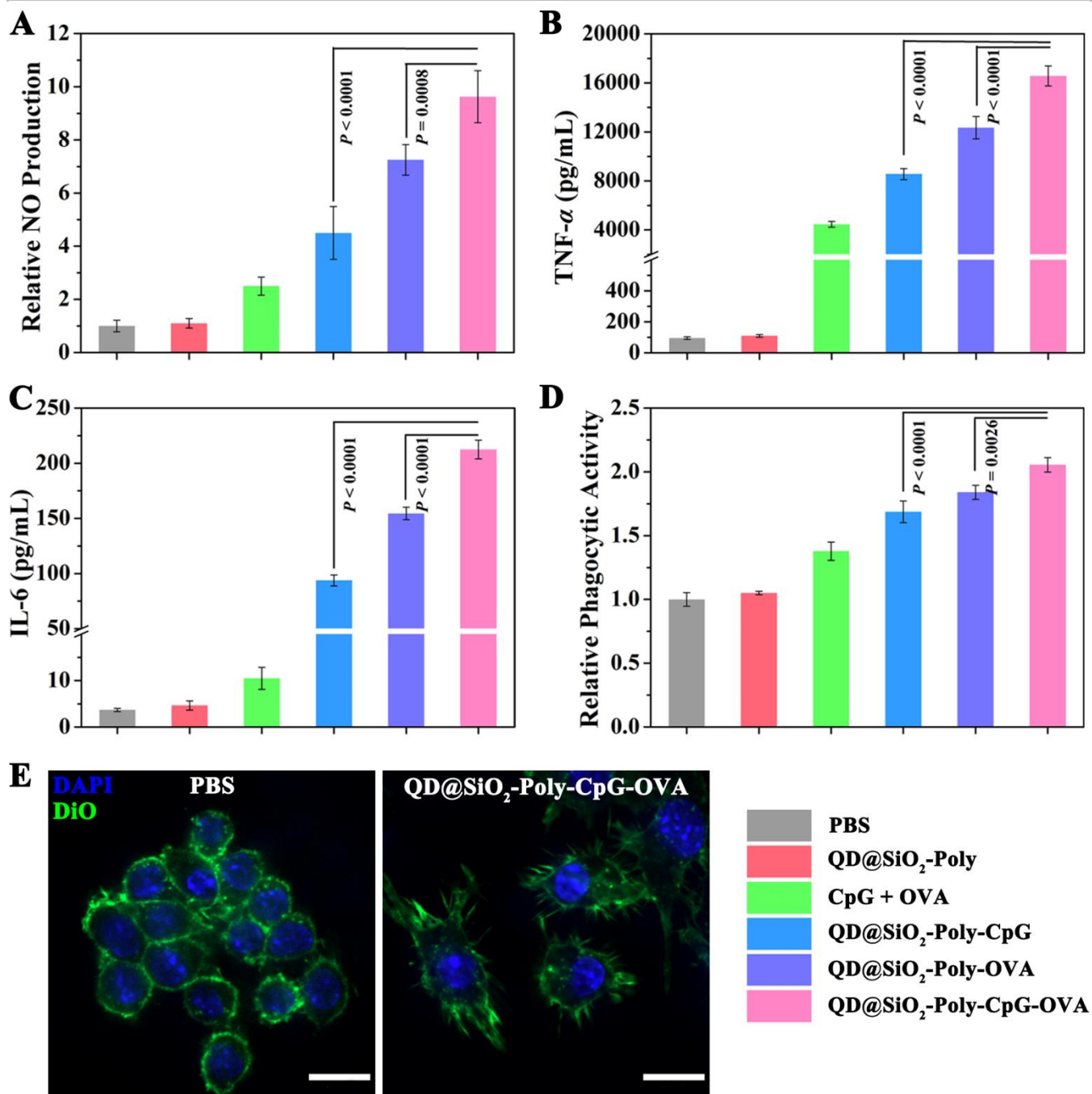


Figure S18. *In vitro* immunoactivation by nanovaccines. (A) Relative NO production detected by Griess reagents ($n = 4$, mean \pm SD). (B and C) ELISA analysis the secretion of TNF- α (B) and IL-6 (C), ($n = 4$, mean \pm SD). (D) Relative phagocytic activity detected by neutral red uptake (compared with PBS group, $n = 4$, mean \pm SD). (E) Confocal images of RAW264.7 cells before and after immunostimulation. Scale bar is 20 μ m. Statistical significance was calculated by one-way ANOVA with the Bonferroni post hoc test.

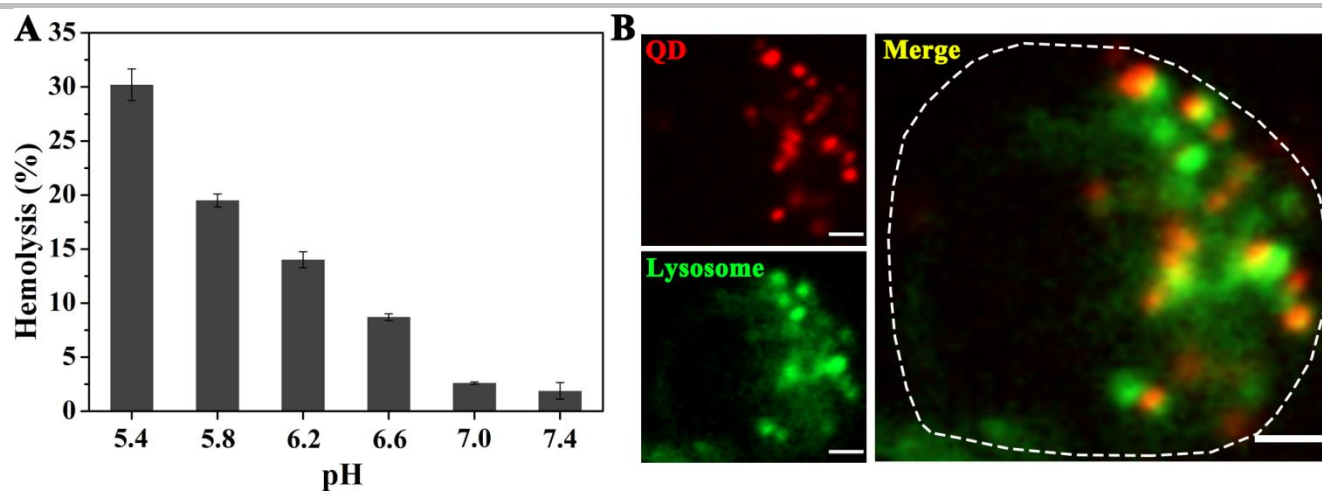


Figure S19. Lysosome escape capability of the nanovaccines. (A) The pH-dependent RBC hemolysis of QD@SiO₂-Poly-CpG-OVA (50 $\mu\text{g/mL}$, $n = 3$, mean \pm SD). (B) CLSM characterization of RAW264.7 cells that were incubated with QD@SiO₂-Poly-CpG-OVA (50 $\mu\text{g/mL}$) for 12 h. Scale bar is 2 μm .

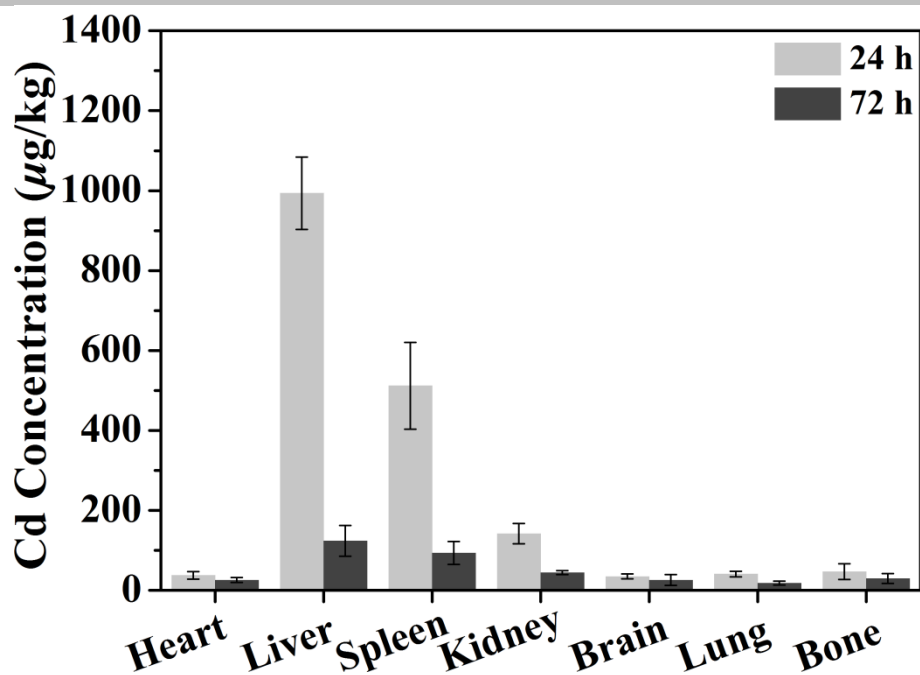


Figure S21. ICP-MS analysis of the organ-accumulated QDs from nanovaccines-injected mice at 24 h and 72 h ($n = 3$, mean \pm SD).

Inductively coupled plasma mass spectrometer (ICP-MS) analysis showed that the residual QDs decreased apparently in the most organs at 72 h post injection, indicating the metabolic clearance of QD-based nanovaccines *in vivo* by the mononuclear phagocytic system (MPS) and the renal clearance pathway.

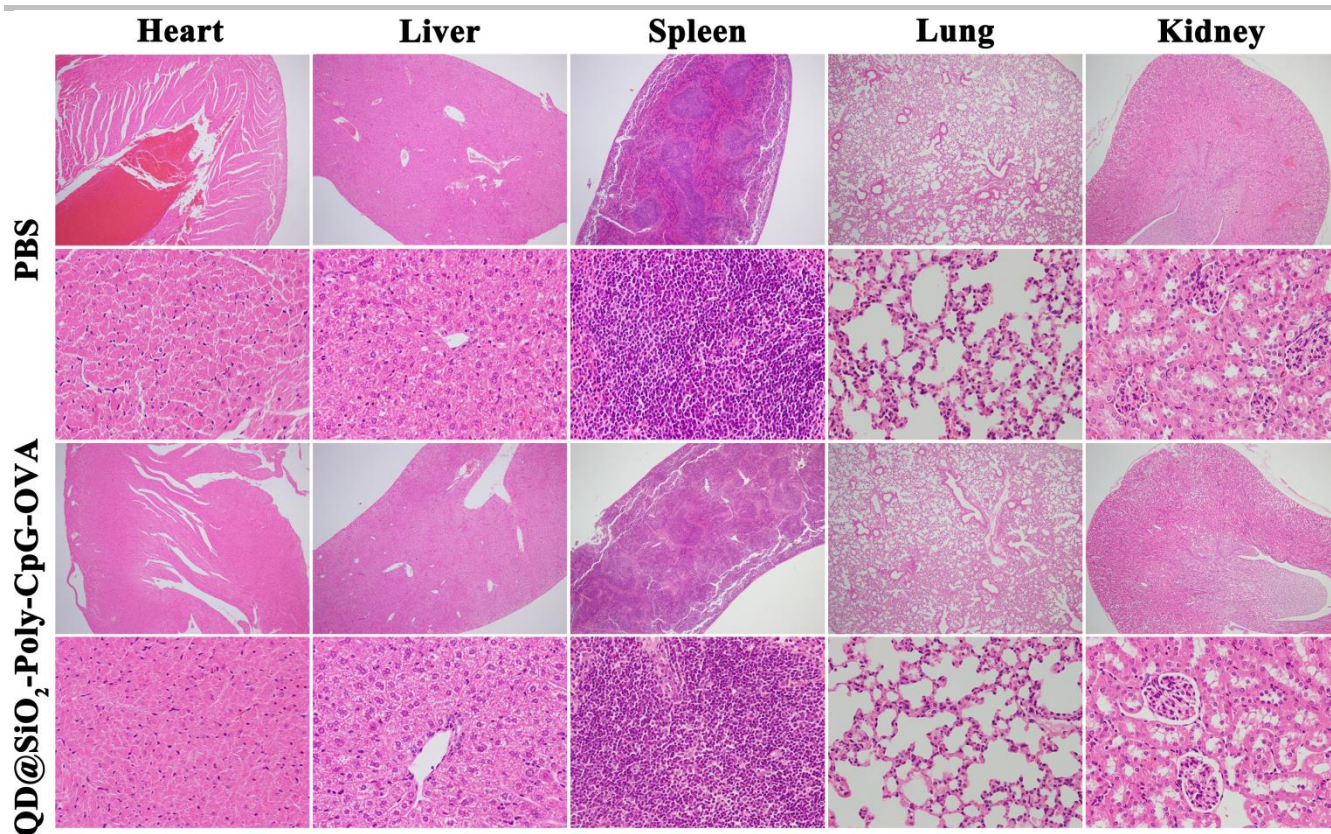


Figure S22. Representative H&E staining of major organs from C57BL/6j mice vaccinated with the indicated materials. Magnification of the images in the first and third row: $\times 40$; Magnification of the corresponding images in the second and fourth row: $\times 400$.

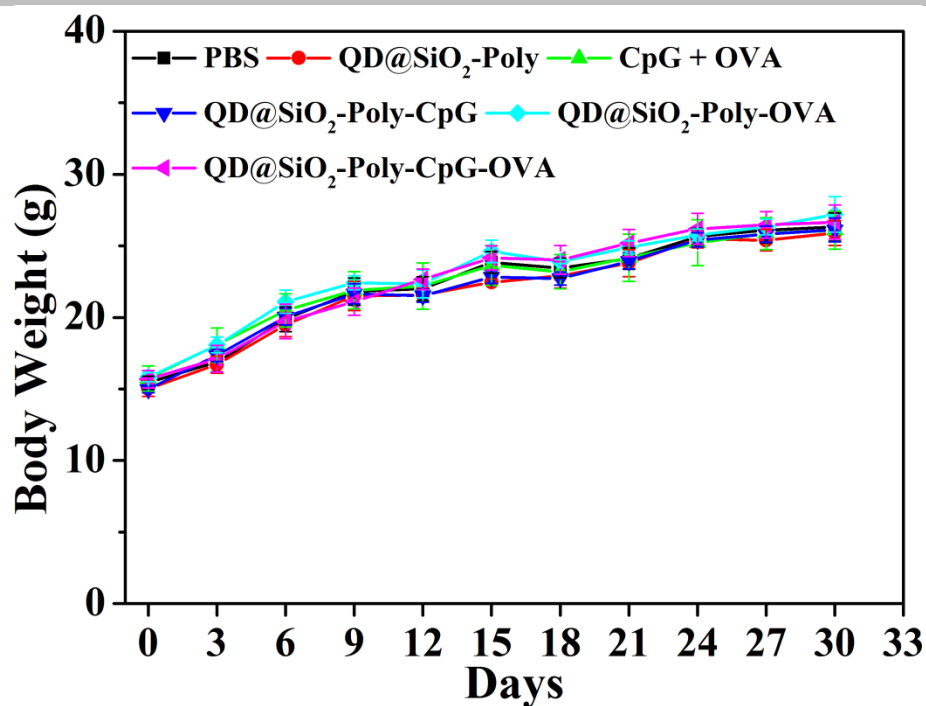


Figure S23. Mean body weights of mice after various indicated treatments in immunogenicity study ($n = 7$, mean \pm SD).

H&E staining images and mean body weights suggested that the nanovaccines induced no obvious toxic side effects to mice (Figure S22, S23).

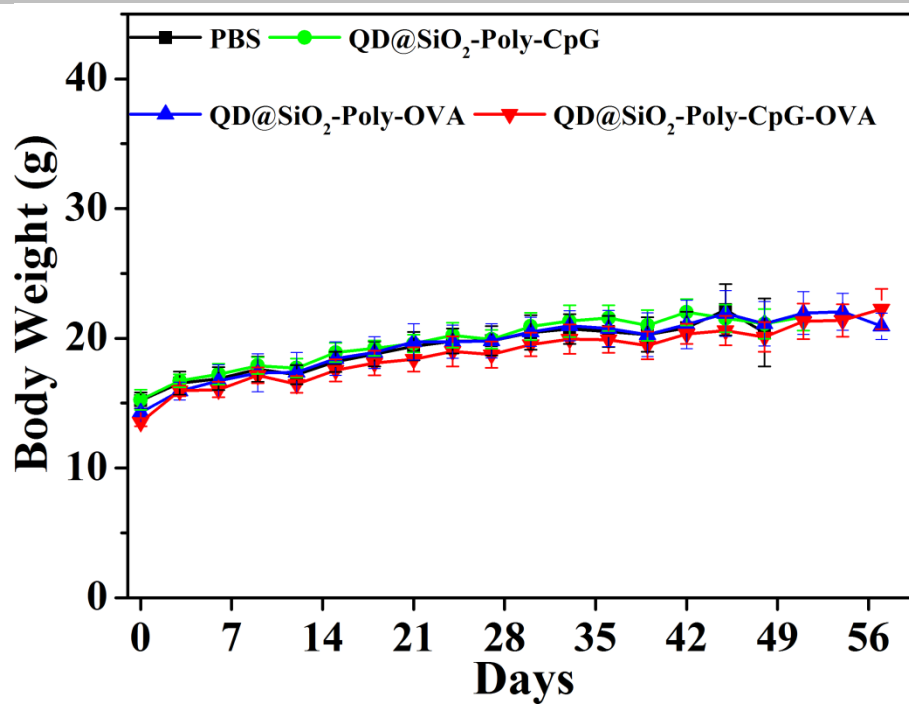


Figure S24. Average body weights of C57BL/6j mice after indicated treatments in prophylactic study ($n = 7$, mean \pm SD).

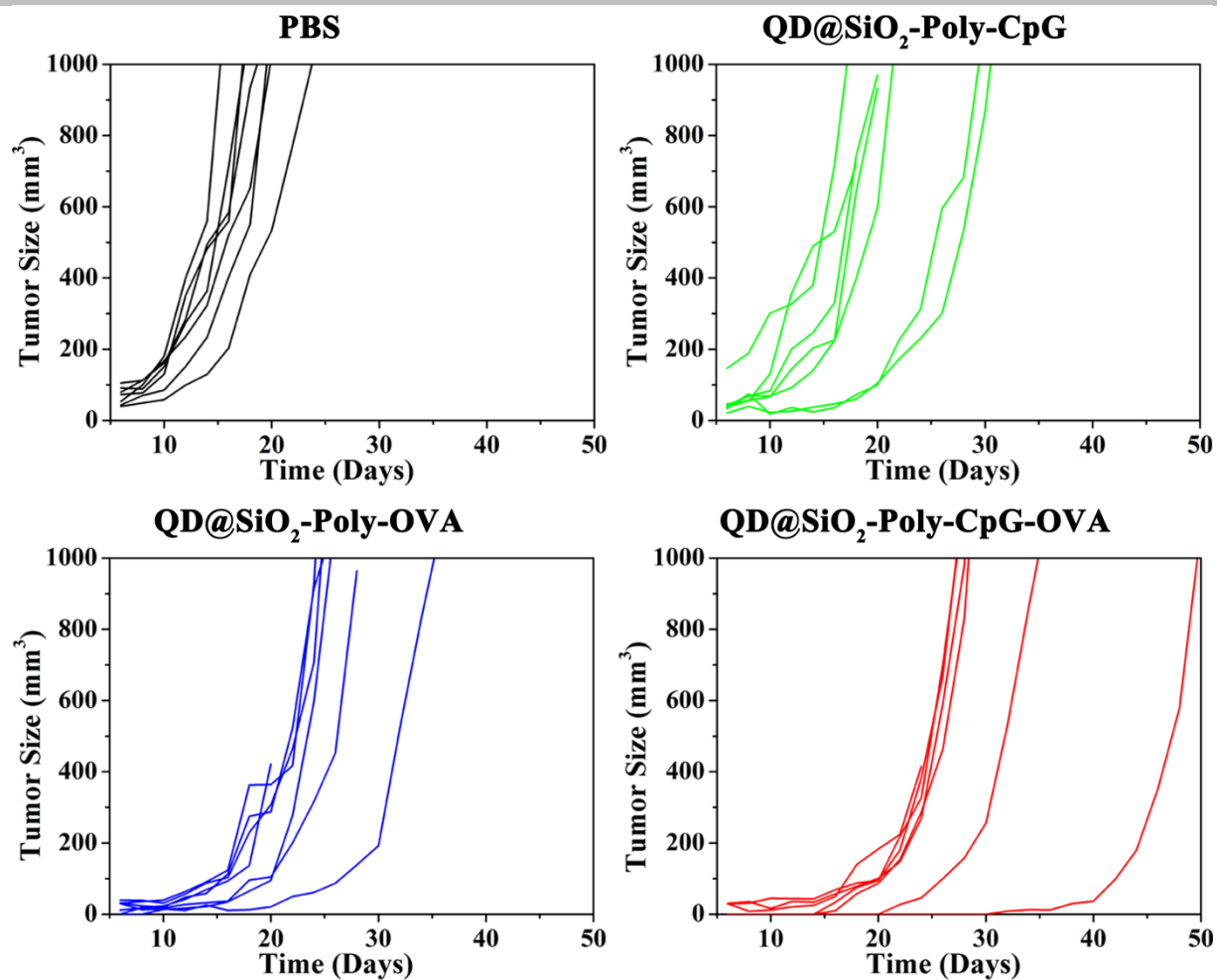


Figure S25. Representative tumor growth plots of C57BL/6j mice after indicated treatments in prophylactic study ($n = 7$).

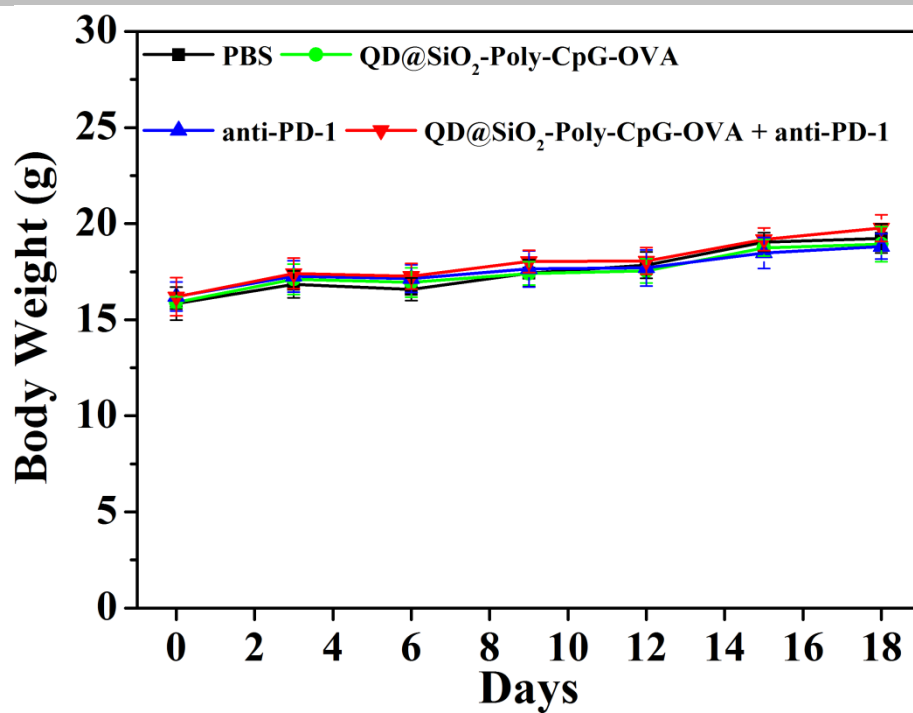


Figure S26. Average body weights of mice after indicated treatments in therapeutic study ($n = 7$, mean \pm SD).

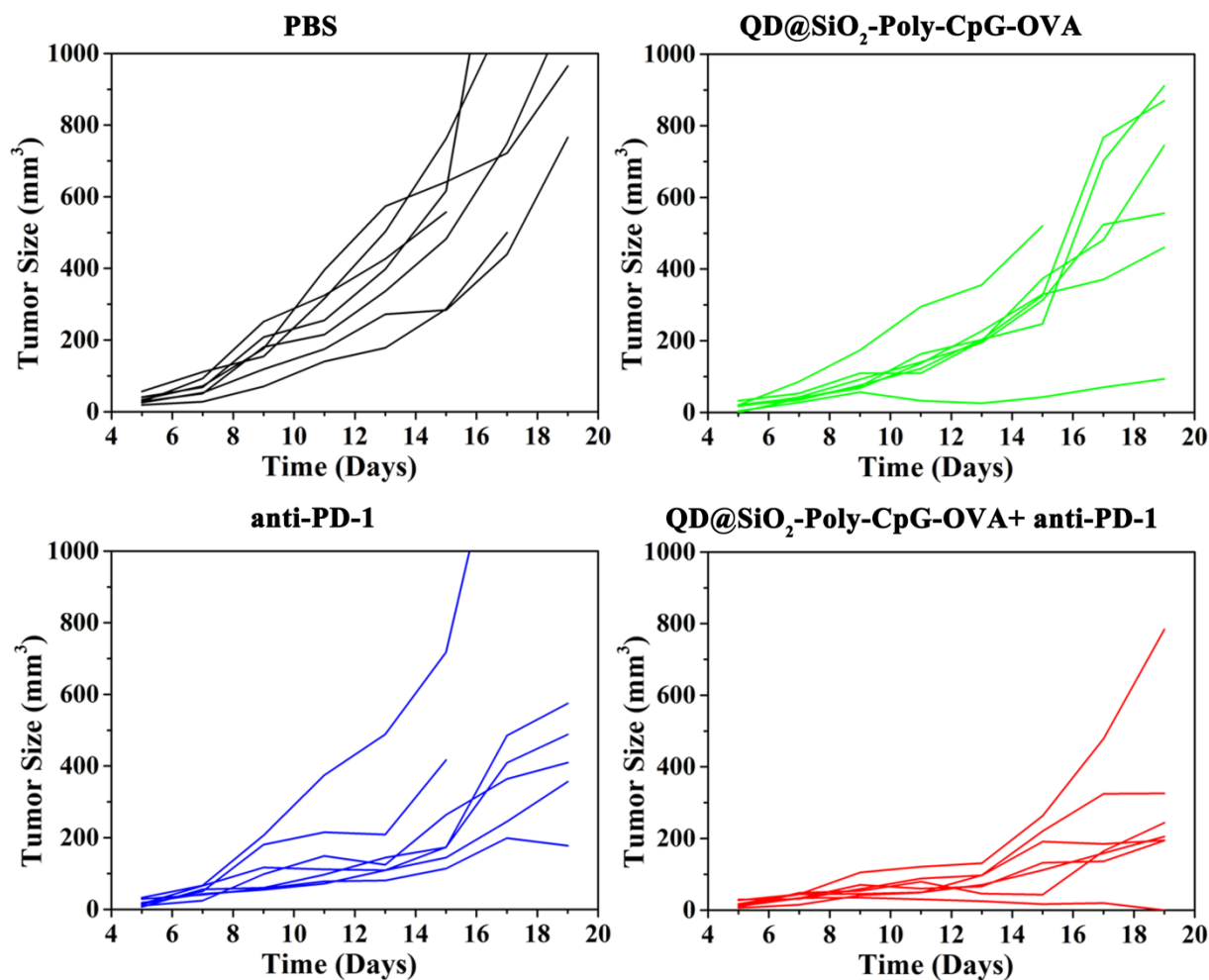


Figure S27. Representative tumor growth plots of C57BL/6j mice after indicated treatments in therapeutic study ($n = 7$).

It was observed that one mouse with the combination treatment had chance to eradicate tumor cells completely.

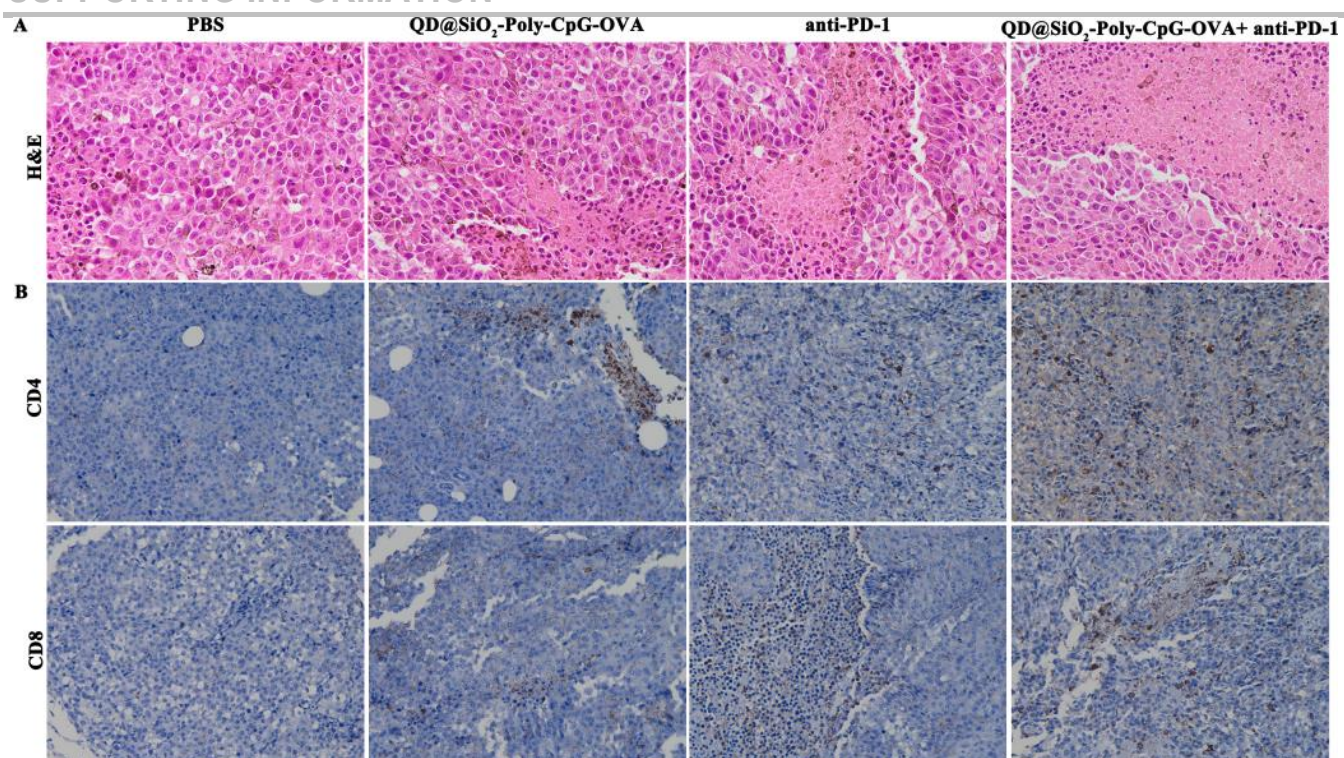


Figure S28. (A) Representative H&E staining of tumor slices. Magnification: $\times 200$. (B) IHC analysis of CD4⁺ T and CD8⁺ T cells in tumor. Magnification: $\times 40$.

Table S1. Quantum yield of the pristine QDs, QD@SiO₂ and QD@SiO₂-Poly, using Rhodamine 6G as a standard.

Sample	Quantum yield (%)
Rhodamine 6G	95.0
Pristine QDs	93.0
QD@SiO ₂	28.4
QD@SiO ₂ -Poly	20.1

References

- [1] S. Q. Wang, C. L. Li, P. Yang, M. Ando, N. Murase, *Colloids Surf., A* **2012**, 395, 24–31.
- [2] J. Sun, F. Liu, W. Yu, Q. Jiang, J. Hu, Y. Liu, F. Wang, X. Liu, *Nanoscale* **2019**, 11, 5014–5020.
- [3] Z. Luo, X. Ding, Y. Hu, S. Wu, Y. Xiang, Y. Zeng, B. Zhang, H. Yan, H. Zhang, L. Zhu, J. Liu, J. Li, K. Cai, Y. Zhao, *ACS Nano* **2013**, 7, 10271–10284.
- [4] Wang, Q. Xu, Z. Ye, H. Liu, Q. Lin, K. Nan, Y. Li, Y. Wang, L. Qi, H. Chen, *ACS Appl. Mater. Interfaces* **2016**, 8, 27207–27217.
- [5] V. Delplace, J. Nicolas, *Nat. Chem.* **2015**, 7, 771–784.
- [6] J. T. Wilson, S. Keller, M. J. Manganiello, C. Cheng, C. C. Lee, C. Opara, A. Convertine, P. S. Stayton, *ACS Nano* **2013**, 7, 3912–3925.
- [7] A. M. Georgoudaki, K. E. Prokopec, V. F. Boura, E. Hellqvist, S. Sohn, J. Ostling, R. Dahan, R. A. Harris, M. Rantalainen, D. Klevebring, M. Sund, S. E. Brage, J. Fuxe, C. Rolny, F. Li, J. V. Ravetch, M. C. Karlsson, *Cell Rep.* **2016**, 15, 2000–2011.